5. Relaxometry and Laplace NMR

- Distributions of relaxation times
- Distributions of diffusion coefficients
- Diffusive diffraction
- Compact magnets
- Well-logging NMR
- 2D Laplace NMR
- Depth profiling
- Applications to materials characterization

B. Blümich, *Essential NMR*,
https://doi.org/10.1007/978-3-030-10704-8_5

Acquiring Distributions of Relaxation Times

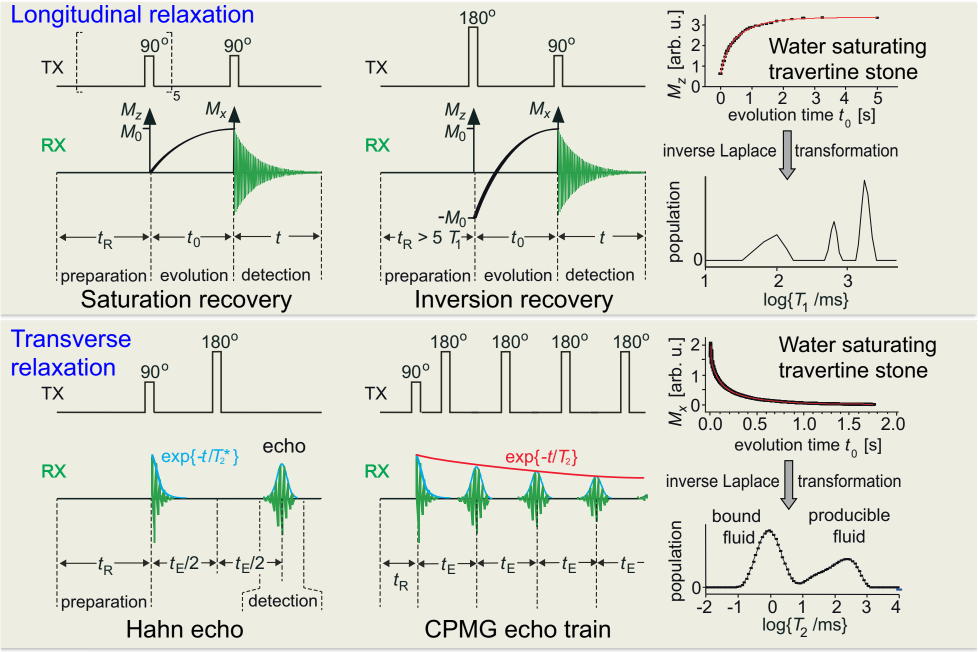

From B. Blümich in: R.A. Mayers, ed., *Enc. Anal. Chem.*, **John Wiley**, Chichester, 2016, a9458, Fig. 13 with permission

NMR Relaxometry

- *Relaxation times* and *diffusion coefficients* can be measured in inhomogeneous magnetic fields by analyzing signal decay and build-up in the *time domain*
- *Inhomogeneous fields* are inexpensive to generate with *permanent magnets*
- The fields of permanent magnets are low (up to 2 T) compared to those of most superconducting NMR magnets (up to 24 T)
- NMR relaxometry with compact low-field instruments was commercialized by Bruker in 1973 for food analysis and not much later by Oxford Instruments
- It is used to test the physical properties of materials, because relaxation times and self-diffusion coefficients report on the rotational and translational molecular motion and not the chemical structure
- Longitudinal relaxation is measured with the *inversion recovery sequence* and the *saturation recovery sequence*
- Transverse relaxation in liquids is measured with the *Hahn echo* and the *CPMG sequence*. In solids it is measured with the *solid echo* and Ostroff-Waugh (*OW4*) sequences, which use 90° instead of 180° refocusing pulses
- In simple liquids, T_1 and T_2 relaxation is mono-exponential
- In multi-component mixtures such as emulsions and fluids in porous media, the relaxation signal can be approximated by a sum of exponential functions
- This can be inverted to a relaxation-time distribution by operations similar to *inverse Laplace transformation*
- This is why *time-domain NMR* is often also called *Laplace NMR*

Fluids in Porous Media

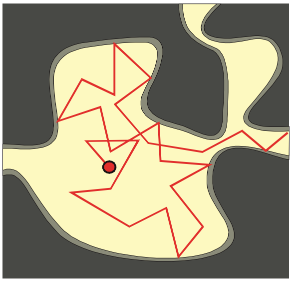

- The signal amplitude is proportional to *porosity* at full fluid saturation
- The longitudinal relaxation rate $1/T_1$ and the transverse relaxation rate $1/T_2$ are enhanced by *wall relaxation*
- The *transverse relaxation rate* is affected by self diffusion in applied and in *internal gradients*
- The molecular *self-diffusion* length is confined by the pore diameter

Relaxation of fluids in in porous media:

$$\frac{1}{T_2} = \frac{1}{T_{2,\mathrm{bulk}}} + \rho_2 \frac{S}{V} + \frac{D\,(\gamma\, G\, t_E)^2}{12}$$

$$\frac{1}{T_1} = \frac{1}{T_{1,\mathrm{bulk}}} + \rho_1 \frac{S}{V}$$

S: surface area
V: pore volume
ρ: surface relaxivity
t_E: echo time
D: apparent diffusion coefficient

Restricted diffusion in fluid-filled pores:

$$\frac{D}{D_0} = 1 - \frac{4}{9\sqrt{\pi}} \frac{S}{V} \sqrt{D_0\,\Delta} + O(\Delta)$$

D: apparent diffusion coefficient
D_0: bulk diffusion coefficient
Δ: diffusion time

Relaxation and Diffusion

- In fluid-filled *porous media*, relaxation and diffusion reveal essential material properties of fluid and matrix, which can readily be measured by ^{1}H NMR
- The signal amplitude is proportional to the amount of fluid in the sensitive volume, i.e. to the *fluid saturation* for partially saturated porous media and the *porosity* for fully saturated porous media
- The pore walls confine the diffusion paths and enhance the relaxation rates of the fluid molecules in the pores
- In the *fast diffusion limit* the relaxation rate is proportional to the *surface-to-volume ratio*, i.e. the relaxation time reports *pore size*
- Contrary to the longitudinal relaxation rate, the transverse relaxation rate is affected by translational diffusion in inhomogeneous fields with a gradient G
- The *field gradient* can arise from the inhomogeneity of the applied field and from *susceptibility differences* due to the heterogeneity of the porous medium
- Information about the *pore size* is also obtained from the restrictions in molecular self-diffusion imposed by the pore walls
- NMR relaxation and self-diffusion signals are inverted to *distributions of relaxation rates* and *distributions of apparent diffusion coefficients* identifying in a porous medium, for example, *bound fluid* and *producible fluid*
- Such distributions from fluid-saturated porous media are interpreted in terms of *pore-size distributions*, which are evaluated for *porosity*, *permeability*, and *fluid typing* in *well-logging NMR*

Gradient Echo

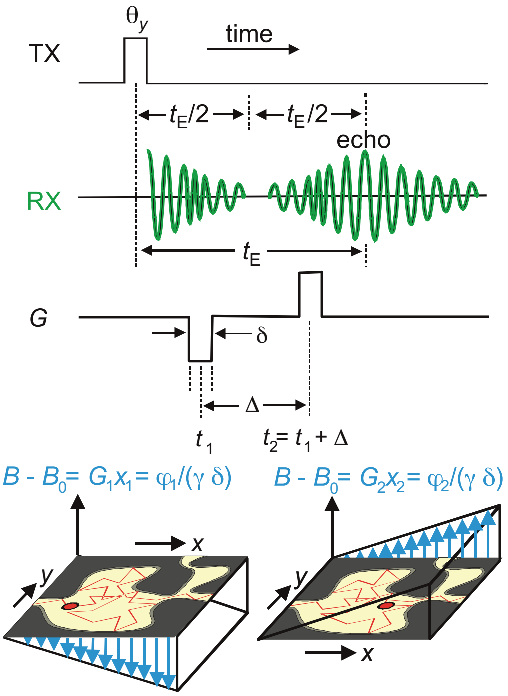

Measuring displacement from diffusion or flow

NMR with pulsed gradient fields: PFG NMR (pulsed field-gradient NMR)

Measuring Diffusion

- Like velocity, *diffusion* is measured in terms of *displacement* $R = r_2 - r_1$ within a given time window, where r is the position of the molecule
- Position is encoded by the phase $\varphi = \gamma\, G\, r\, \delta = k\, r$ of the transverse magnetization evolving for a time δ in an *inhomogeneous field*, which is preferably linear with a constant gradient G. Here k is the position wave number
- Displacement is measured by the phase $\Delta\varphi = k_1 r_1 + k_2 r_2 = k\,(r_2 - r_1) = q\, R$ accumulated with two gradient pulses at different times having the same wavenumber magnitude k but opposite signs, where q is the wave number for displacement
- In such an *anti-phase gradient-pulse pair* the position wave number $k = k_1 + k_2$ vanishes after the second gradient pulse so that position is not encoded in the signal phase and the gradient-pulse pair is said to generate a *gradient echo*
- If all spins move coherently in a pulsed linear gradient-field, all acquire the same phase difference, which appears as a *phase shift of the echo*
- If the spins diffuse randomly, positive and negative phase shifts cancel on average, and the echo amplitude is attenuated according to $M_{xy}(t) = M_{xy}(0)$ $\exp\{-t_E/T_2\} \times \exp\{-q^2 D(\Delta - \delta/3)\}$, where D is the *self-diffusion coefficient* and Δ the *diffusion time*
- The transverse magnetization $M_{xy}(t) = M_0 \int P(R) \exp\{-\mathrm{i}\, q\, R\}\, \mathrm{d}R$ of an ensemble of spins diffusing different distances R during the diffusion time without relaxation is determined by the Fourier transform of the *probability density* $P(R)$ *of displacements*, which is known as the *propagator* in NMR

Pulse Sequences for Diffusion NMR

PFG NMR with a Hahn echo

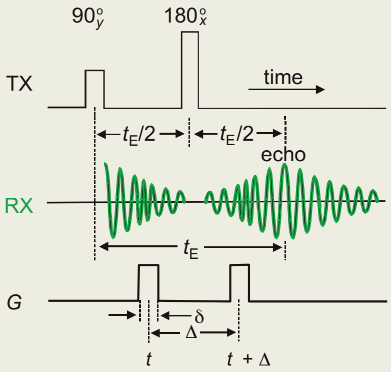

Distortions of the magnetic induction field ***B*** by susceptibility differences:
$\Delta\chi = \chi_{pore} - \chi_{matrix}$

Estimation of the *internal gradient* of a pore:
$G_{int} \approx \Delta\chi\, H / r_{pore}$
H: vacuum magnetic field

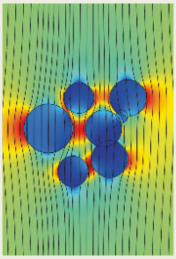

CPMG sequence in a time-invariant gradient field $B - B_0 = G\, r$ and the effective gradient G_{eff}

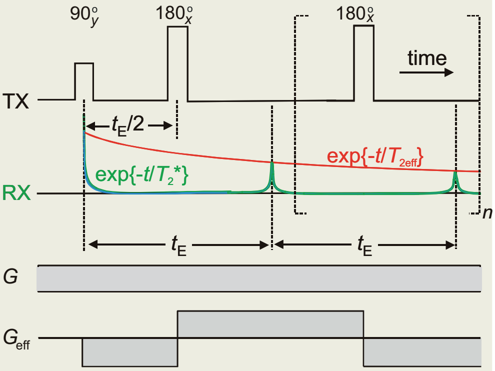

Time-Invariant Gradient Fields

- If the field gradient results from the sensor or *magnetic susceptibility differences* in the object it is time-invariant and an echo can be generated by rf pulses
- In the maximum of the Hahn echo and the stimulated echo, the dephasing of magnetization components from magnetic fields that are inhomogeneous across the sample is refocused unless the spins are moving
- The refocusing rf pulse of the Hahn echo changes the sign of all *precession phases* $\varphi = k\, r$ accumulated before
- This is equivalent to a sign change of all position-encoding gradients active before, and one can write the time variation in terms of the *effective gradient* G_{eff}, which gives the same result but without refocusing rf pulses
- For example, identical gradient pulses before and after the refocusing pulse in a Hahn echo to encode *diffusion* and *coherent flow* are equivalent to an echo with the effective gradient
- In a CPMG train applied in a linear field $B(r) - B_0 = G\, r$ all odd echoes refocus dephasing from different positions, and all even echoes in addition also refocus dephasing from coherent displacement
- The decay of the *CPMG echo envelope* due to *relaxation* and *diffusion* is given by $M_{xy}(t) = M_{xy}(0) \exp\{-n\, t_E / T_2\} \exp\{-q^2 D\, n\, t_E / 3\}$
- In *stray-field NMR*, the rf field is inhomogeneous and all rf pulses are selective, so that the flip angles vary across the sample
- Then the CPMG echoes are mixed Hahn and stimulated echoes, and T_2 becomes an *effective relaxation time* T_{2eff}, which is a mixture of T_1 and T_2

Effects of Displacement

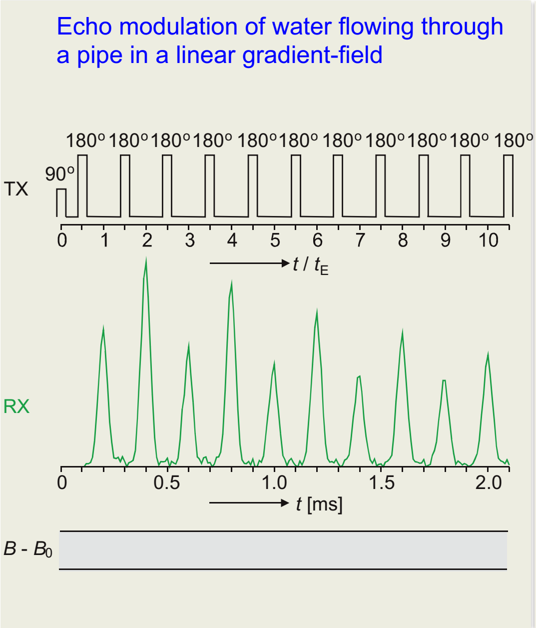
Echo modulation of water flowing through a pipe in a linear gradient-field

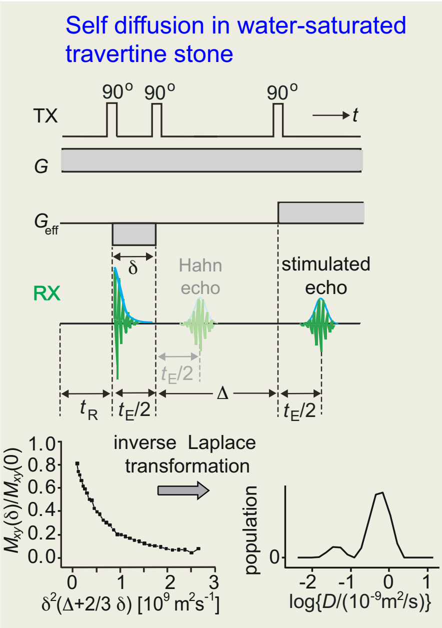
Self diffusion in water-saturated travertine stone

Displacing Spins

- The paths of spins being displaced during a time shorter than T_1 can be probed by different NMR methods
- In a *stimulated echo* sequence, the echo amplitude is attenuated from displacement by *diffusion D* in a constant gradient and by relaxation following $M_{xy}(t) = ½\, M_{xy}(0) \times \exp\{-q^2 D\, (\Delta + t_E/3\,)\} \times \exp\{-\Delta/T_1\} \times \exp\{-t_E/T_2\}$
- Other than diffusion, *laminar flow* through a pipe is coherent leading to a phase shift in addition to the attenuation of the echo from diffusion and relaxation
- As $q = \gamma\, G\, t_E/2$, the logarithm the CPMG *echo attenuation* depends linearly on $t_E{}^3$ for free diffusion, and D can be determined from the slope of $\ln\{M_{xy}\}$
- To improve the sensitivity of diffusion measurements, the diffusion-attenuated echo may be refocused several times with echo time t_{E2} and the echo sum be detected for a systematic variation of the first echo time t_{E1}
- For sufficiently short echo times t_{E2} in the CPMG *detection period*, signal loss in the *CPMG echo train* due to diffusion is suppressed
- Then, without the summation, the scheme gives a 2D data set of Hahn-echo attenuation from diffusion versus T_2 relaxation decays
- The T_2 relaxation can be neglected in the *diffusion filter* for strong gradients, and a D-T_2 correlation map is obtained by *2D inverse Laplace transformation*
- In porous media, diffusion is restricted, so that the signal attenuation by diffusion is lowered, and that from relaxation is enhanced due to *wall relaxation*

Waves in Space

$$M_{xy}(\mathbf{r}) = M_{xy}(\mathbf{0}) \exp\{\mathrm{i}\, \mathbf{k}\, \mathbf{r}\}$$
$$= M_{xy}(\mathbf{0}) [\cos\{\mathbf{k}\, \mathbf{r}\} + \mathrm{i} \sin\{\mathbf{k}\, \mathbf{r}\}]$$

$\mathbf{r}$: space vector
$\mathbf{k}$: wave vector
$\mathbf{k}\, \mathbf{r} = \varphi$: phase

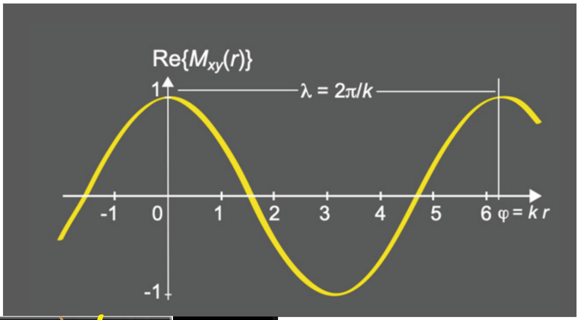

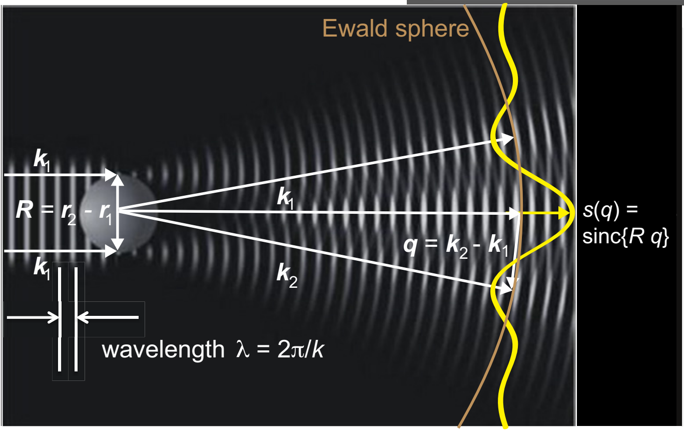

Diffraction

The interference patterns of light, X-rays, neutrons, or electrons report the Fourier transform of the distribution of scattering centers

Distributions of Velocities and Displacements

- According to the phase table in chapter 4, the magnetization component moving with constant velocity v through a linear gradient-field is given by $M_{xy}(t) = M_{xy}(0) \exp\{-t/T_2\} \exp\{-\mathrm{i}\varphi_{11}\}$
- Here $\varphi_{11}(t) = \gamma \int_0^t G(t')\, t'\, \mathrm{d}t'\, v = \gamma \int_0^t G(t')\, t'\, \mathrm{d}t'\, R/\Delta$, where R is the distance travelled during time Δ and $G(t)$ is the *effective gradient*
- For coherent flow $\varphi_{11}(t) = q_v(t)\, v$. In the case of a diffusing magnetization component, the notation of Callaghan applies, and $\varphi_{11}(t) = q(t)\, R$ with $k = q$
- For many magnetization components the transverse magnetization is the integral over all velocities v or displacements R, $M_{xy}(t) = (1/V) \int M_{xy}(v) \exp\{-\mathrm{i}\, q_v\, v\}\, \mathrm{d}v = (1/V) \int M_{xy}(R) \exp\{-\mathrm{i}\, q\, R\}\, \mathrm{d}R$
- $M_{xy}(v)/V$ is the *velocity distribution* and $M_{xy}(R)/V$ the *displacement distribution*
- For constant magnetization density, $M_{xy}(R)/(M_0\, V) = P(R)$ is the probability density of displacements, also known as the *propagator*
- For diffusion, R depends on the diffusion time Δ and so does the propagator
- For free diffusion, the propagator is a *Gauss function*, which broadens with increasing diffusion time, $P(R,\Delta) = (4\pi\, D\, \Delta)^{-3/2} \exp\{-R^2/(4\, D\, \Delta)\}$, the variance $\langle R^2 \rangle = 2\, D\, \Delta$ of which defines the *mean diffusion length* $\langle R^2 \rangle^{1/2} = (2\, D\, \Delta)^{1/2}$
- For *restricted diffusion* in identical pores, the propagator is the *auto-correlation function of the pore shape* in the fast diffusion limit, and *diffraction* peaks are observed in the NMR signal

Diffraction

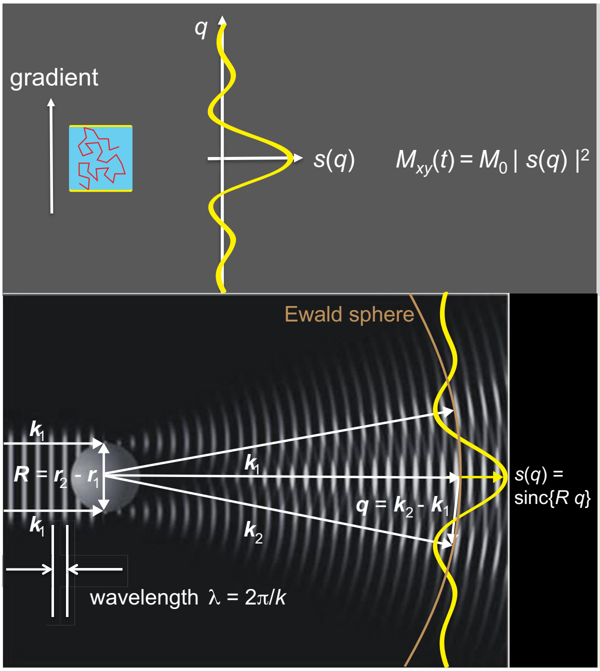

Diffusive diffraction of nuclear magnetization waves

In the fast diffusion limit the transverse magnetization is the magnitude square of the Fourier transform of the pore-shape function: $M_{xy}(t) = M_0 \mid s(q) \mid^2$

Diffraction of conventional waves

The interference pattern is described by the magnitude square of the Fourier transform $s(q)$ of the distribution of scattering centers: $I(q) = I_0 \mid s(q) \mid^2$

In the first diffraction maximum: $q = 2\pi/R$

Diffusive Diffraction

- The *propagator* $P(R)$ can be written as integral over all initial positions r_1 of the product of the probability density $S(r_1)$ of finding a spin at r_1 and the conditional probability density $S(r_1,r_2,\Delta)$ of finding it at $r_2 = r_1 + R$ some time Δ later,
$$P(R) = \int S^*(r_1)\, S(r_1, r_1{+}R, \Delta)\, \mathrm{d}r_1$$
- At long diffusion time Δ, $S(r_1, r_1{+}R, \Delta) = S(r_2)$. Then, with $q\,R = k\,(r_2 - r_1)$, $M_{xy}(q) = M_0 \int P(R) \exp\{-\mathrm{i}\, q\, R\}\, \mathrm{d}R$, and rewriting $P(R)$ one obtains
$$\begin{aligned} M_{xy}(q) &= M_0 \int\!\!\int S^*(r_1)\, S(r_2)\, \mathrm{d}r_1 \exp\{-\mathrm{i}\, k\,(r_2 - r_1)\}\, \mathrm{d}(r_2 - r_1) \\ &= M_0 \int\!\!\int S^*(r_1)\, S(r_2) \exp\{-\mathrm{i}\, k\, r_2\} \exp\{\mathrm{i}\, k\, r_1\}\, \mathrm{d}(r_2 - r_1)\, \mathrm{d}r_1 \\ &= M_0 \int S^*(r_1) \exp\{\mathrm{i}\, k\, r_1\}\, \mathrm{d}r_1 \int S(r_2) \exp\{-\mathrm{i}\, k\, r_2\}\, \mathrm{d}r_2 \\ &= M_0\, s^*(k)\, s(k) = M_0 \mid s(k) \mid^2 = M_0 \mid s(q) \mid^2 \end{aligned}$$
- This states, that the transverse magnetization measured in a diffusion experiment reports the magnitude square of the Fourier transform of the probability density $S(r)$ of finding spins at position r
- For fluid-filled pores, $S(r)$ is the normalized projection of the pore shape along the gradient direction. It is commonly called the *pore-shape function*
- In the limit of fast diffusion or long Δ, the transverse magnetization is proportional to the magnitude square of the Fourier transform of the pore-shape function

Compact Magnets for Laplace NMR

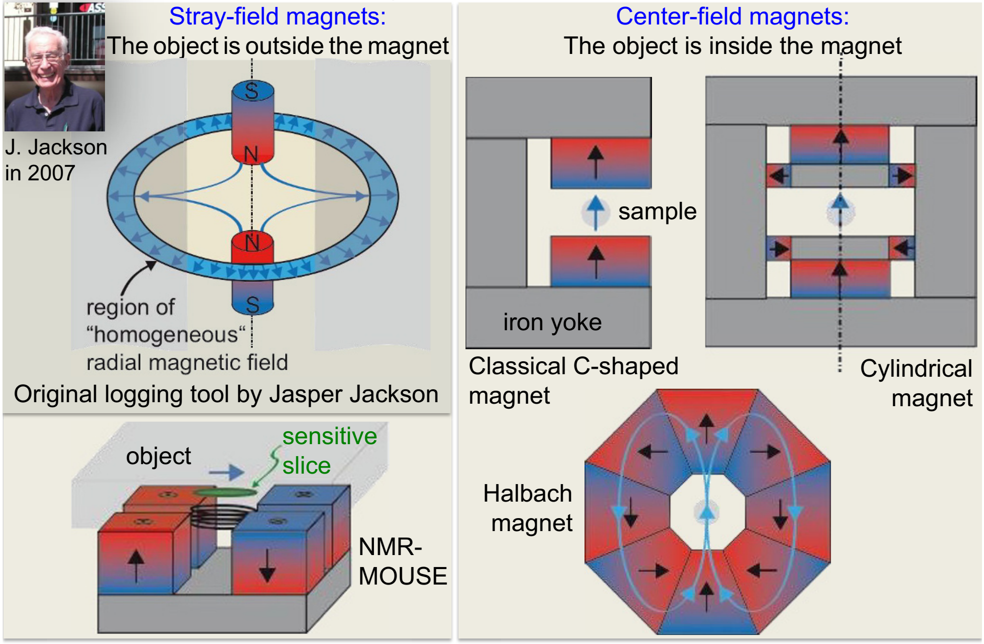

From B. Blümich, C. Rehorn, W. Zia, in: J. Anders, J. Korvink, eds., *Micro and Nano Scale NMR*, **Wiley-VCH**, Weinheim, 2018, Fig. 1.7 with permission

Permanent Magnets for NMR Relaxometry

- The first NMR experiments were done with *electromagnets* and later on also with permanent magnets at ^{1}H frequencies from 20 MHz up to 90 MHz
- Permanent magnets were hard to shim and drift with temperature so that compact permanent magnets were mostly used for relaxation and diffusion measurements in the past
- There are two basic types of magnets for NMR, stray-field magnets and center-field magnets
- *Center-field magnets* accommodate the sample inside, so that the sample size is limited by the diameter of the magnet opening
- The classical geometry is C-shaped, while mirrored C-shapes and cylinder shapes provide better field homogeneity due to higher symmetry
- *Halbach magnets* are particularly efficient and ideally are without stray field
- *Stray-field magnets* produce fields that enter the object from one side
- They were first used for *well logging* to be inserted into the hole of an oil well and to acquire signal from the fluids in the borehole wall
- Compact stray-field instruments were subsequently developed mostly for moisture measurements in buildings and porous media
- The *NMR-MOUSE* (Mobile Universal Surface Explorer) is a small stray-field sensor, which collects the signal from a flat sensitive slice outside the magnet
- It can be used to measure depth profiles into the surface of arbitrarily large objects by changing the distance between sensor and object

Concepts of NMR Logging

Wireline logging

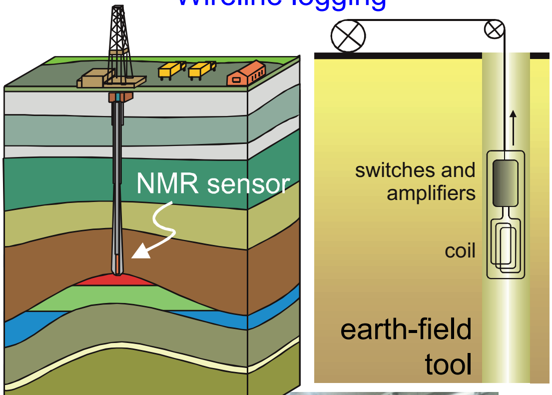

Logging while drilling:
directional drilling

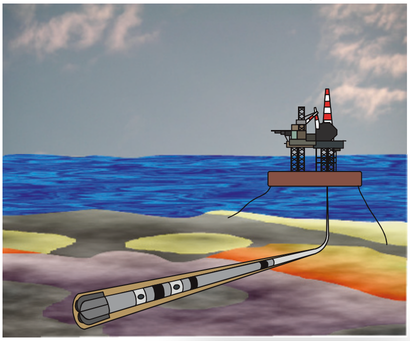

Assembly of a wireline logging tool (Changping, 2011)

Bob Kleinberg built the first commercial NMR logging tool. In the photo he explains a wireline log (Cambridge, USA, 2008)

NMR Well Logging

- Early on NMR was of interest for *well logging*. Russell Varian had the idea in the early 1950's, and oil companies like Chevron, Mobil, Texaco, Borg-Warner and Schlumberger started to study fluids in porous rock
- The first generation nuclear magnetic logging tools operated in the earth's magnetic field. Later on J. Jackson introduced permanent magnets
- Since the magnet is inside the sample and not the sample inside the magnet, this type of stray-field NMR is also called *inside-out NMR*
- Due to the inhomogeneous stray field and field-gradients inside the rock pores induced by susceptibility differences, the NMR signal is acquired with CPMG-like multi-echo sequences
- Since 1995 NMR logging tools are operated by service companies. *Halliburton* calls their tool MRIL (Magnetic Resonance Imaging Log) and *Schlumberger* calls it CMR (Combinable Magnetic Resonance tool)
- The tools of the first and the second generations were operated in *wireline mode* after drilling and measured the NMR information while being pulled up through the hole
- The third generation tools are designed for *logging while drilling*. They are part of the drill string and suitable for *directional drilling*
- Some logging-while-drilling tools explore the original magnet geometry proposed by Jasper Jackson

Sensor Designs

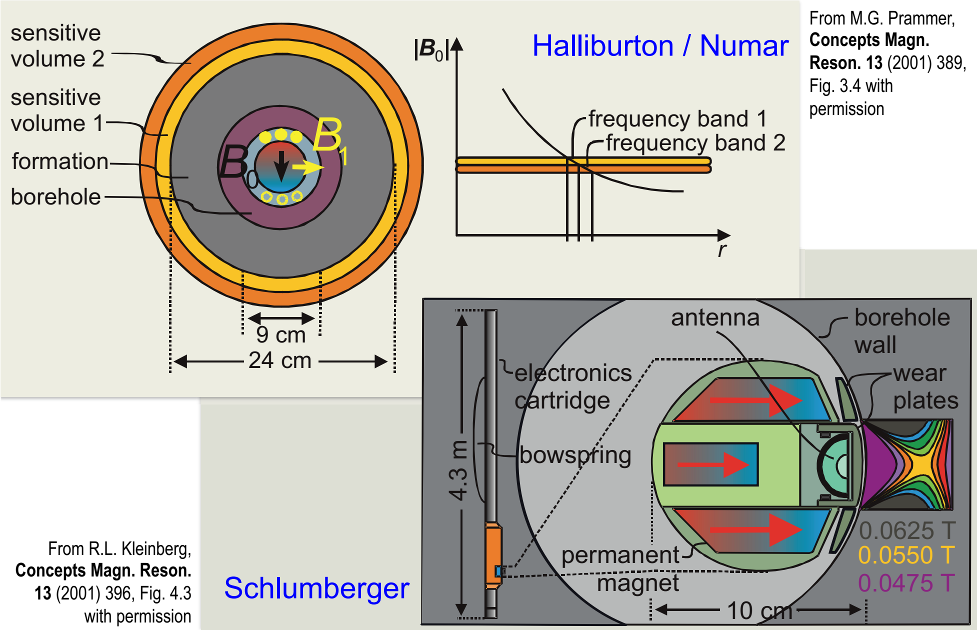

From M.G. Prammer, **Concepts Magn. Reson. 13** (2001) 389, Fig. 3.4 with permission

From R.L. Kleinberg, **Concepts Magn. Reson. 13** (2001) 396, Fig. 4.3 with permission

NMR Logging Tools

- The *earth-field tool* of the first generation used a strong DC current through the coil to magnetize the protons and then used the same coil for detection
- The *deadtime* was 30 ms, and the fluid molecules exposed to fast *wall relaxation* could not be measured
- Only *free fluid* could be measured, but not *porosity*. Oil, water, and bore-hole fluid could not be distinguished
- By fitting the sensors with magnets, several problems could be solved:
  - The NMR frequency increased from 2 kHz to about 1 MHz so that the deadtime was shortened and the sensitivity increased
  - The signal dependence on the sensor orientation in the earth's field is avoided
  - The sensitive volume can be localized inside the borehole wall away from the borehole fluid
- The *Jackson tool* has a sensitive volume in the shape of an annulus, which is narrow in the axial direction. Measurements with such a sensor moving along the bore-hole are difficult as the spins find little time to be polarized
- The *Halliburton/Numar tool* has transverse dipolar B_0 and B_1 fields, which are largely perpendicular to each other at all locations. The field magnitude at a given radius is constant along the circumference. The radial gradient helps to select signal from different shells by tuning to different frequencies
- The *Schlumberger tool* provides an axially extended sweet spot in one angular segment at some distance away from the sensor

NMR of Fluids in Porous Media

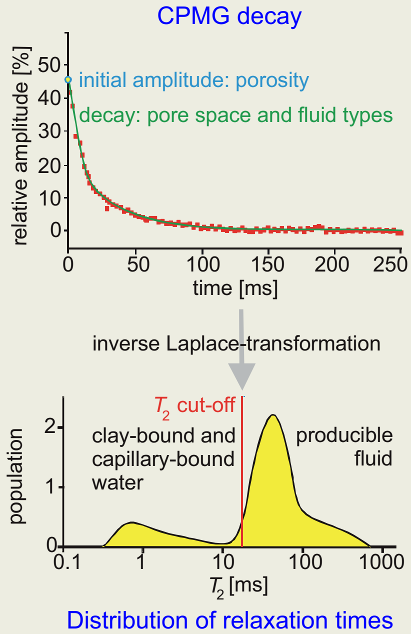
CPMG decay

Distribution of relaxation times

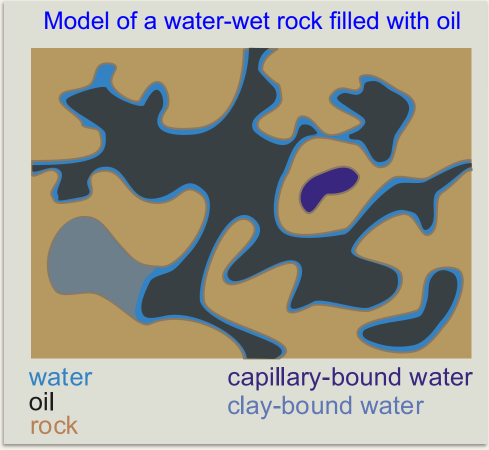
Model of a water-wet rock filled with oil

The initial amplitude of the CPMG decay is the integral of the T_2 distribution

Formation Evaluation by NMR

- Modern *NMR logging tools* acquire data from more than 5 cm deep into the formation of the bore-hole wall
- Typically the transverse magnetization decay from fluid-filled pores is measured as the envelope of a Carr-Purcell-Meiboom-Gill (*CPMG*) *echo train*
- Its amplitude provides mineralogy-independent *porosity* $\Phi = V_{\text{pores}}/V_{\text{rock}}$
- The *distribution of relaxation times* T_2 is obtained from the echo-train decay envelope by *inverse Laplace transformation*
- The area under the distribution curve is the amplitude of the CPMG signal
- A model-bound analysis of the relaxation time distribution yields
  - *irreducible water saturation* from *clay-bound* and *capillary-bound water*
  - amount *of producible fluid*
  - *permeability estimates*
  - *hydrocarbon type*
  - *oil-viscosity estimates*
- Porosity is estimated traditionally from density values determined by *gamma-ray scattering* or *neutron scattering*, applying formation-dependent corrections
- NMR porosity is formation independent unless the formation is magnetic
- Advanced *multi-dimensional Laplace methods* provide more detailed information, e.g. they can separate signals from oil and water and characterize *pore connectivity*

NMR Porosity and Relaxation in Pores

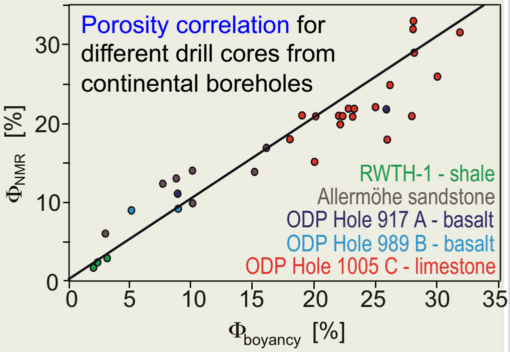

From J. Arnold, C. Clauser, R. Pechnig, S. Anferova, V. Anferov, B. Blümich, **Petrophysics 47** (2006) 306, Fig. 4 with permission

Diffusion of magnetization M_z in porous media

within the pore: $D\nabla^2 M_z(\mathbf{r},t) - \dfrac{M_z(\mathbf{r},t)}{T_{1,\text{bulk}}} = \dfrac{\partial M_z(\mathbf{r},t)}{\partial t}$

at the interface: $\mathbf{n} D \nabla M_z(\mathbf{r},t) + \rho M_z(\mathbf{r},t) = 0$

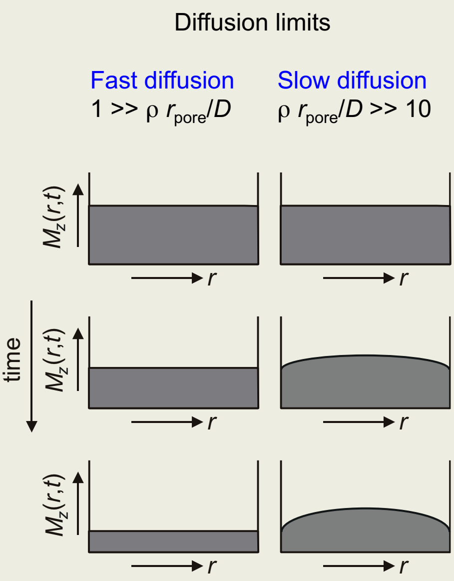

Diffusion limits

Fast diffusion
$1 \gg \rho r_{\text{pore}}/D$

Slow diffusion
$\rho r_{\text{pore}}/D \gg 10$

Porosity and Surface Relaxation

- The *porosity* Φ is directly determined from the signal amplitude of the fluid in the rock normalized to the signal amplitude of bulk water and corrected for the *hydrogen index* HI, which corresponds to the relative spin density of the fluid
- The fluid molecules diffuse inside the pores of the rock matrix
- To reduce the signal loss within the *deadtime* of the instrument, low measuring fields are advantageous because lower fields induce smaller *field inhomogeneity* at interfaces resulting from *magnetic susceptibility differences* so that signal attenuation from *diffusion in internal gradients* of the pores is low
- NMR porosity scales well with porosity determined by *buoyancy*
- The *longitudinal magnetization* $M_z(\mathbf{r},t)$ follows the *diffusion equation* with the *bulk relaxation time* $T_{1,\text{bulk}}$ within a pore, and in the direction along the normal ***n*** of the wall it relaxes with the *surface relaxivity* ρ
- A normal mode analysis leads to the slow and the fast diffusion limits
- In the *fast diffusion limit*, the relaxation rate scales with the *surface-to-volume ratio* S/V, where $S/V = 3/r_{\text{pore}}$ for spherical pores, and the transverse magnetization decay is mono-exponential
- The fast diffusion limit is assumed to be valid in most applications of NMR to *well logging*
- In the *slow diffusion regime*, the magnetization decay is multi-exponential for a single type of pore and depends on the *pore geometry*

Relaxation-Time Distributions and Pore Size

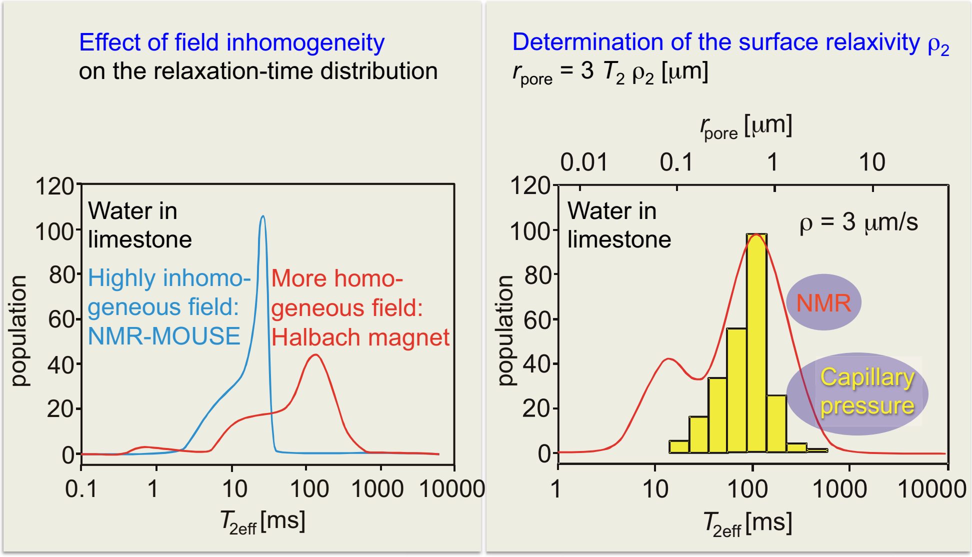

Effect of field inhomogeneity on the relaxation-time distribution

Determination of the surface relaxivity ρ_2

$r_{pore} = 3\,T_2\,\rho_2$ [µm]

From J. Arnold, C. Clauser, R. Pechnig, S. Anferova, V. Anferov, B. Blümich, **Petrophysics 47** (2006) 306, Figs. 5. 6 with permission

Surface Relaxation

- The *surface relaxivity* ρ links *pore size* and *relaxation time*
- It is determined by matching the *relaxation-time distribution* from NMR with the *pore-throat distribution* determined e.g. by differential capillary pressure measurement such as *mercury intrusion porosimetry*
- The pore-throat distribution scales with the derivative of the *capillary pressure* (CP) curve versus fluid saturation
- The assumptions are that the pore radii are proportional to the throat radii and that all pores have the same surface relaxivity
- By comparing T_1 and T_2 relaxation-time distributions, one finds, that most rocks exhibit T_1/T_2 ratios between 1 and 2.5 with a most probable value of 1.65 at 2 MHz. That value becomes larger at higher measuring fields
- Deviations may arise at short relaxation times from contributions to T_2 by diffusion in internal gradients if the echo time is not chosen short enough
- The shapes of the NMR relaxation-time distributions depend only weakly on pressure and temperature
- For immobile molecules T_{2eff} derived from a multi-echo decay in a strongly inhomogeneous magnetic field is prolonged by scrambling of longitudinal and transverse magnetization components from resonance-offset related flip-angle distributions
- For mobile molecules T_{2eff} is shortened by diffusion in field gradients

Producing Water from Porous Media

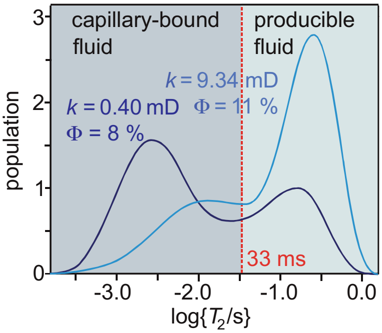

T_2 distributions of Allermoehe sandstones: The bound water decreases with increasing permeability k and macro porosity Φ of the rock

From S. Anferova, V. Anferov, J. Arnold, E. Talnishnikh, M.A. Voda, K. Kupferschläger, P. Blümler, C. Clauser, B. Blümich, **Magn. Reson. Imag. 25** (2007) 474, Fig. 6 with permission

Drying of water saturated pietra di Noto measured with the NMR-MOUSE at 3 mm depth

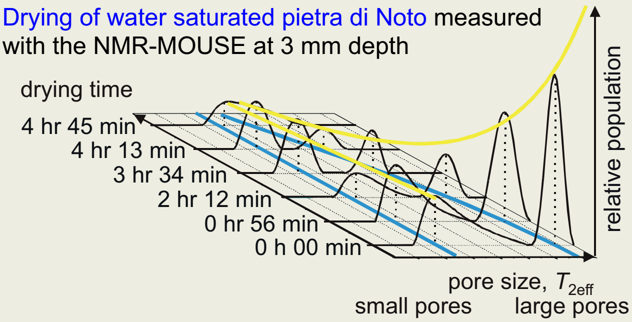

Estimating permeability

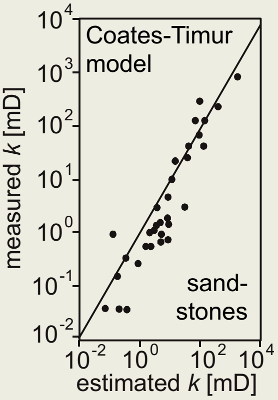

From C.-C. Huang, *Estimation of Rock Properties by NMR Relaxation Methods*, **Thesis**, Rice University, Houston, 1997, Fig. 6.5.2.2 with permission

Fluid Production from Porous Media

- When drying a water-wet rock, the large pores lose water first and the small pores later, i.e. the irreducible water remains in the small pores
- A *relaxation-time cut-off* serves to estimate *bound water* from *producible fluid*
- The T_2 cut-off for water is 33 ms in sandstones and 92 ms in carbonates
- For *crude oil* with a broad distribution, the relaxation times of bound water and producible oil may overlap, but the fractions may be distinguished by diffusion measurements
- The flow velocity v of a fluid with dynamic viscosity η through a porous medium in a pressure gradient $\Delta p/\Delta x$ is determined by the *permeability* k, $v = k/\eta\ \Delta p/\Delta x$. It is measured in Darcy, where $1\ \text{Darcy} = 1\ \text{D} = 0.987\times10^{-12}\ \text{m}^2$
- The permeability $k = C\, d^2$ is poportional to the square of the effective pore diameter d, where C is a constant relating to the flow paths
- It is estimated from the relaxation-time distribution following models of the form $k = a\, \Phi^4\, T_{2,k}^{\,2}$, where, depending on the model, $T_{2,k}$ is an average relaxation time derived from all or parts of the relaxation-time distribution
- The *Kenyon model* fits best for 100% brine saturated rock, the *Coates-Timur model* applies to hydrocarbons, and the *Chang model* to vuggy carbonates
- The Chang model has been improved to accommodate a large range of permeabilities by introducing a tortuosity-dependent weight
- The *tortuosity* $\tau = D_0/D_\infty$ is the ratio of the bulk self-diffusion coefficient to the apparent self-diffusion coefficient at long diffusion time $\Delta \rightarrow \infty$

Example of a Gas-Well Log

Tracks 1 – 3 are conventional logs,
tracks 5 – 11 are NMR logs

- Track 1: CAL caliper, GR natural gamma ray, SP spontaneous potential
- Track 2: DT acoustic travel time, ZDEN density, CNCF neutron porosity
- Track 3: RS shallow resistivity, RML middle resistivity, RD deep resistivity
- Track 4: Depth in meter with 1:250 scale
- Track 5: Porosity profiles for bins of the relaxation-time distribution from 2048 ms via 128 ms to 4 ms
- Track 6: Permeability from a customized Coates model
- Track 7: T_2 distribution from an echo-train measurement with a long polarization time t_0
- Track 8: T_2 distribution from an echo-train measurement with a short polarization time t_0
- Track 9: T_2 distribution of the echo difference from acquisitions with $t_{0,\text{long}}$ and $t_{0,\text{short}}$
- Track 10: Total porosity, effective porosity, capillary bound water and clay bound water determined from different relaxation components
- Track 11: Porosities for gas, oil, producible water and bound water determined by advanced analysis

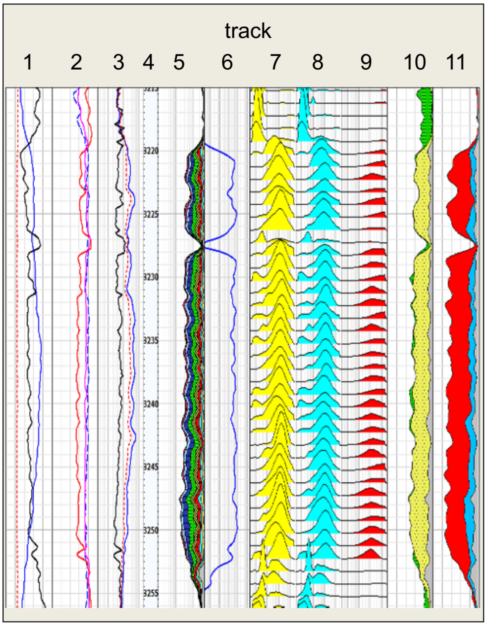

Courtesy of L. Xiao, China University of Petroleum, Changping, China

Elementary Well Logging

- Elementary NMR *well logging* is based on the analysis of *CPMG decays* and associated *distributions of relaxation times* from fluid saturated pores
- The amplitude of the total signal estimates the porosity
- The amplitude of the slowly relaxing part estimates the amount of *producible fluid* (free fluid index FFI) corresponding to the integral of the relaxation time distribution to the right of the relaxation cut-off
- The amplitude of the rapidly relaxing components estimates the amount of capillary and clay-bound water also called the bulk volume irreducible BVI corresponding to the integral of the relaxation time distribution to the left of the relaxation cut-off
- *Permeability* is estimated from the porosity following different models
- Information about the hydrocarbon type is obtained from T_1 *weights* introduced by different *polarization times* t_0 and from *diffusion weights* introduced by different *echo times* t_E when the signal is acquired in the presence of a field gradient
- All NMR data are interpreted in the context of other logging data from measurements of *electrical resistivity*, *gamma-ray scattering*, *neutron scattering*, etc.
- Detailed measurements by *2D Laplace NMR* and other more advanced methods are performed in *logging-while-drilling* applications and on core samples in the laboratory
- Well logging data are validated by data from laboratory studies

Hydrogen Index and Relaxation of Dead Oils

$$\mathrm{HI} = \frac{{}^1\text{H density of sample}}{{}^1\text{H density of water}} = \left(\frac{n_\mathrm{H}\,\rho}{M_\mathrm{w}}\right)\Big/\left(\frac{2\times 1\ \text{g}}{18\ \text{g cm}^3}\right)$$

n_H : number of protons in the molecule
ρ : fluid density
M_w: molecular weight

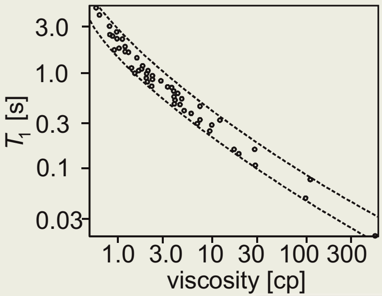

T_1 of crude oils versus viscosity at different temperatures

From R.J.S. Brown, **Nature 189** (1961) 387, Fig. 1 with permission

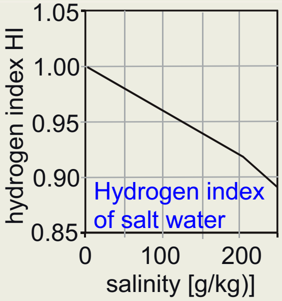

Hydrogen index of salt water

From R.L. Kleinberg, H.J. Vinegar, **The Log Analyst 37** (1996) 20, Fig. 4 with permission

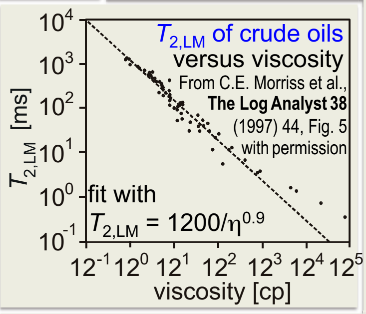

$T_{2,\mathrm{LM}}$ of crude oils versus viscosity

From C.E. Morriss et al., **The Log Analyst 38** (1997) 44, Fig. 5 with permission

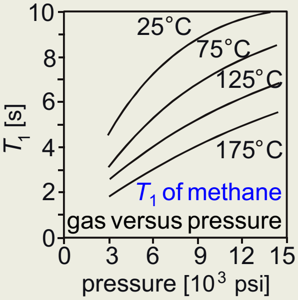

T_1 of methane gas versus pressure

From K.-J. Dunn, D.J. Bergman, G.A. Latorraca, *Nucl. Magn. Reson. Petrophys. Log. App.*, **Pergamon Press**, Oxford, 2002, Fig. 3.10 with permission

NMR Properties of Fluids in Porous Media

- The NMR signals from fluids in porous media relate to the bulk fluids and the pore space. The signal decay is affected by *bulk relaxation*, *wall relaxation*, and by *diffusion* across regions with different magnetic field strengths
- The *signal amplitude* scales with the total number of protons within the sensitive volume. At full fluid saturation it reports formation *porosity*
- Natural fluids saturating rock are water of variable salinity, gas, and oil
- The *water salinity* ranges from zero to full saturation with mostly NaCl
- The most important gas in well logging is *methane*
- When the oil is free of gas, it is called *dead oil*, otherwise it is called *live oil*
- Live oils exist at elevated pressures and temperatures below the bubble point. Their relaxation times depend on the the gas/oil ratio
- *Synthetic oils* are used in *drilling mud* and can mix with reservoir fluids
- The amount of a fluid is quantified from the NMR signal amplitude via the proton density relative to that of water. This quantity is the *hydrogen index HI*
- Since the beginning of the relaxation curve is hidden within the *dead time* of the instrument, *HI* determined by NMR is an *apparent hydrogen index*
- Most rocks are water wet, so that the detected water signal exhibits relaxation times shortened by *wall relaxation*
- Because the relaxation time of bulk water is long (1 to 3 s), the bulk-water signal can be suppressed with short repetition times

Bulk Diffusion of Water, Gas, and Oil

Self-diffusion coefficient of water versus temperature

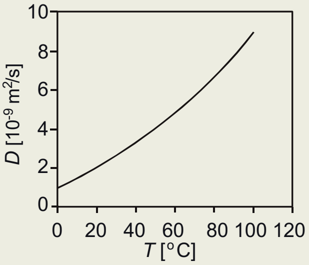

From, D.J. Bergmann, G.A. La Torraca, *Nucl. Magn. Reson. Petrophys. Logg. App.*, **Pergamon Press**, Oxford, 2002, Fig. 3.13 with permission

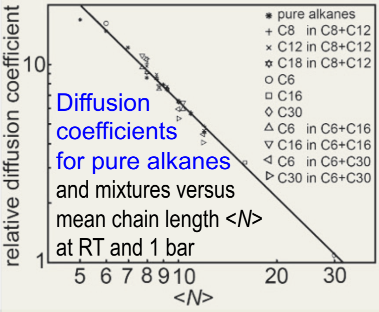

Diffusion coefficients for pure alkanes and mixtures versus mean chain length <*N*> at RT and 1 bar

From D.E. Freed, L. Burcaw, Y.-Q. Song, **Phys. Rev. Lett. 94** (2005) 067602, Fig. 2a with permission

Self-diffusion coefficient of methane versus temperature at different pressures

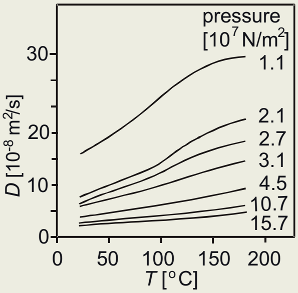

From R.L. Kleinberg, H.J. Vinegar, **The Log Analyst 37** (1996) 20, Fig. 14 with permission

Molecular weight distributions from diffusion measurements

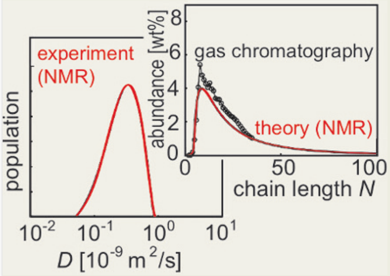

From D.E. Freed, L. Burcaw, Y.-Q. Song, **Phys. Rev. Lett. 94** (2005) 067602, Fig. 3 with permission

Bulk Relaxation and Diffusion

- In water-wet rock the oil is not in direct contact with the pore wall, so that T_1 and T_2 of oil in the pores are the same as in bulk
- For pure compounds both relaxations are mono-exponential, but *crude oils* consist of many components and exhibit distributions of relaxation times
- From the T_2 distribution $x(T_2)$, the *logarithmic mean relaxation time* $T_{2,\mathrm{LM}}$ is calculated as $\log\{T_{2,\mathrm{LM}}/\mathrm{s}\} = [\Sigma_i\, x_i \log\{T_{2i}/\mathrm{s}\}]/[\Sigma_i\, x_i]$. It scales with the *viscosity*
- For *dead oils* $T_{2,\mathrm{LM}}$ scales linearly with the ratio of viscosity/temperature
- Unlike T_1 of liquids, T_1 of gases is shortened by the *spin rotation interaction*, i.e. the coupling between the proton spins and the field produced by the rotation of the molecule, so that T_1 of gases increases with increasing pressure
- In inhomogeneous fields the magnetization decays by T_2 and diffusion
- The *diffusion of water* (D = 2.23 10^{-9} m^2/s at RT) is insensitive to pressure but sensitive to temperature
- The *diffusion of methane* ($D \approx 10^{-3}$ m^2/s at RT) is much faster than that of water and increases with increasing temperature and decreasing density
- For a melt of linear polymers, the diffusion coefficient $D_i = N_i^{-\nu} A \langle N\rangle^{-\beta}$ of component *i* relates to the average degree <*N*> of polymerization through a power law with degrees of polymerization N_i and exponents ν, β
- The *molecular weight distribution* of the melt is mapped by the distribution of diffusion coefficients, i.e. the chemical composition of crude oil can be mapped by the distribution of a physical NMR parameter

General Scheme for 2D NMR

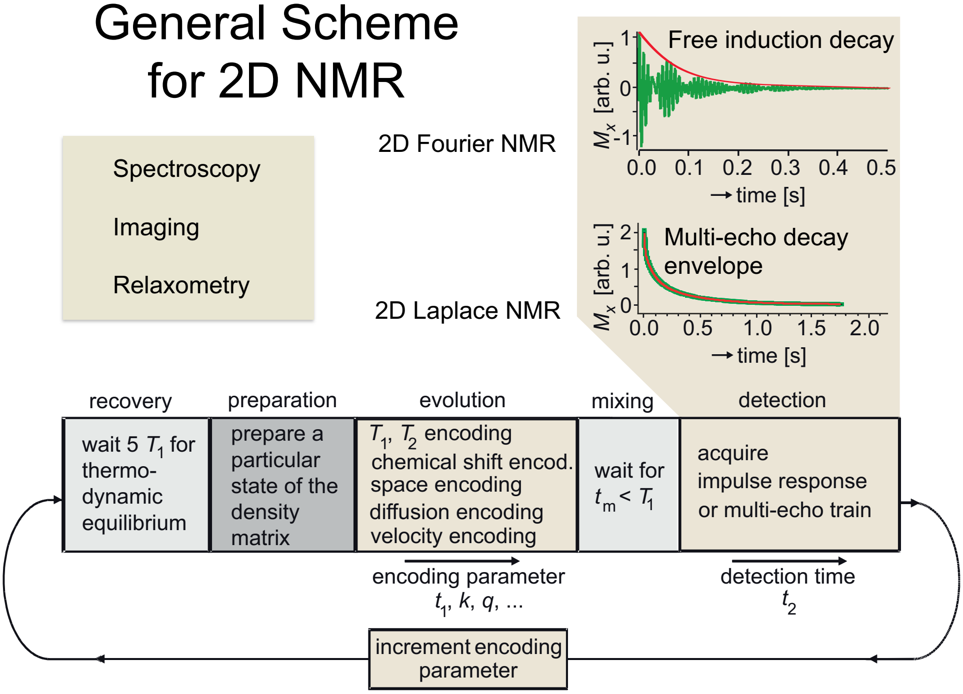

Spectroscopy
Imaging
Relaxometry

2D Fourier NMR
2D Laplace NMR

recovery	preparation	evolution	mixing	detection
wait 5 T_1 for thermo-dynamic equilibrium	prepare a particular state of the density matrix	T_1, T_2 encoding chemical shift encod. space encoding diffusion encoding velocity encoding	wait for $t_m < T_1$	acquire impulse response or multi-echo train

encoding parameter $t_1, k, q, \ldots$

detection time t_2

increment encoding parameter

General Two-Dimensional NMR

- Two-dimensional NMR was introduced for *high-resolution spectrosocpy* and subsequently extended to 3D and *multi-dimensional NMR spectroscopy*
- With the availability of a fast *2D inverse Laplace transformation algorithm,* 2D Laplace NMR became popular
- Similar to the *1D inverse Laplace transformation*, also the 2D inverse Laplace transformation is unstable in the presence of noise and needs to be regularized, so that the transforms are not unique but, depending on the regularization algorithm, they are probable solutions
- The scheme for *2D Laplace NMR* is the same as that for *2D Fourier NMR* including MRI, except that instead of a free-induction decay (FID), a multi-echo decay envelope is recorded during the detection period t_2
- It's amplitude is modulated by the events during the preceding *mixing period*, *evolution period, preparation period* and *recovery period*
- The most popular 2D Laplace experiments are the T_1-T_2 correlation experiment, the T_2-T_2 exchange experiment and the D-T_2 correlation experiment
- *Diffusion-ordered spectroscopy* (*DOSY*) can be understood as a mixed 2D Laplace-Fourier NMR experiment, which correlates distributions of diffusion coefficients with distributions of chemical shifts, i.e. with the NMR spectrum. It is used for chemical identification of components in complex solutions

2D Laplace NMR

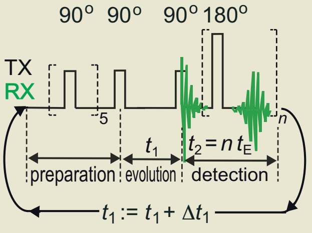

Saturation-recovery - CPMG

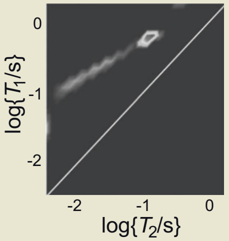

T_1-T_2 correlation map of water saturating Allermöhe sandstone

From S. Anferova, V. Anferov, J. Arnold et al., **Magn. Reson. Imag. 25** (2007) 474, Fig. 9b with permission

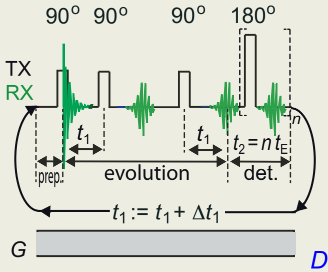

Stimulated echo - CPMG

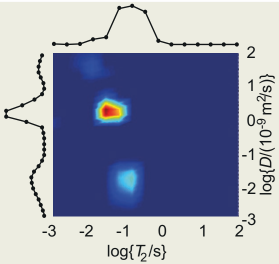

D-T_2 map of oil and water

From B. Blümich, **Trends Anal. Chem. 83** (2016) 2, Fig. 4c with permission

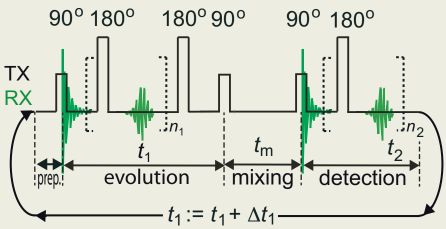

CPMG – wait - CPMG

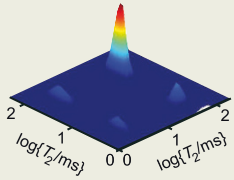

T_2-T_2 exchange map of water saturating nano-porous silica particles

From B. Blümich, **Trends Anal. Chem. 83** (2016) 2, Fig. 4d with permission

Two-Dimensional Laplace NMR

- *Two-dimensional Laplace NMR* concerns correlation maps of *distributions of relaxation times* and *diffusion coefficients*. It can be executed on fluids in *porous media* exhibiting *internal gradients* and even with stray-field instruments
- The signal is detected with a multi-echo sequence giving the T_2 distribution
- With *T_1-T_2 correlation NMR*, T_1 is encoded in the evolution period
- The T_1-T_2 correlation map of water in Allermöhe sandstone reports the impact of diffusion in internal gradients G on the transverse signal decay: Due to diffusive attenuation, the T_1/T_2 ratio varies with pore size $1/(S/V)$
- With *D-T_2 correlation NMR*, D is encoded in the evolution period
- While the relaxation times of oil and water in porous rock overlap on the T_2 scale, the two types of fluid can be separated along the diffusion axis D
- D-T_2 correlation NMR is good for quantifying different fluids such as oil and water in porous media based on differences in diffusion coefficients and T_2
- *T_2 -T_2 exchange NMR* probes diffusion without application of field gradients by molecules diffusing between different relaxation sites
- T_2 is encoded in both, the evolution period and the detection period, which are separated by a *mixing time* t_m
- The exchange map reveals connectivity of pores by diffusion-mediated magnetization transfer between pores similar to *2D NOESY spectroscopy*, which reveals distances between chemical sites by relaxation-mediated magnetization transfer between different chemical groups in molecules

Diffusion-Ordered Spectroscopy

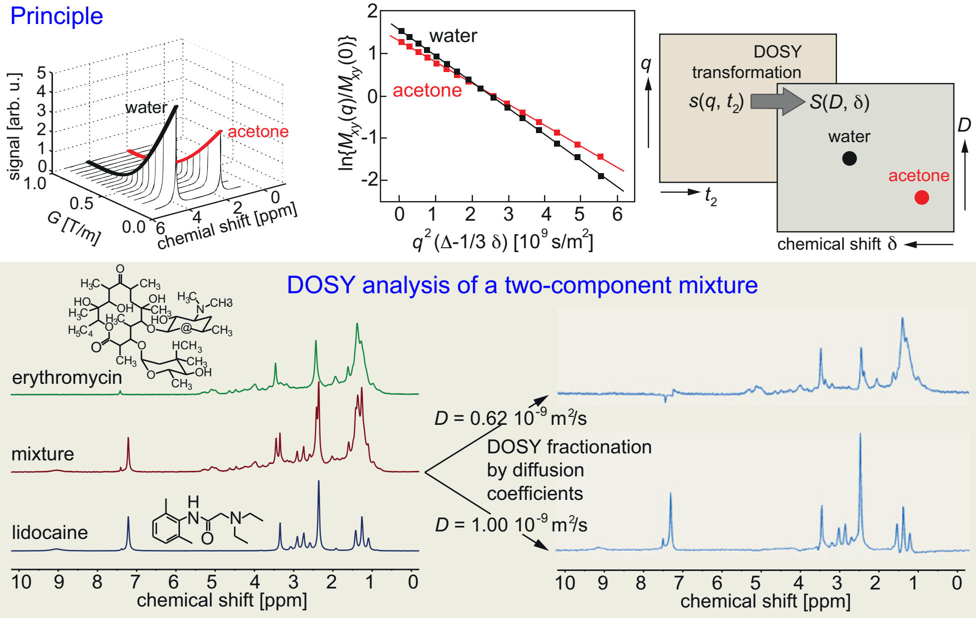

From B. Blümich, **Trends Anal. Chem. 83** (2016) 2, Fig. 4 with permission

2D Fourier-Laplace NMR

- Mixed 2D Fourier-Laplace methods correlate the NMR spectrum with a distribution of relaxation times or diffusion coefficents, where the spectral information is detected directly during t_2
- The most powerful method is *diffusion-ordered spectroscopy* (*DOSY*)
- It separates a crowded spectrum of a multi-component liquid into a set of subspectra of components with similar diffusion coefficients
- In the pulse sequence, the FID is diffusion encoded in the evolution periods of a stimulated echo with two anti-phase field-gradient pulses of amplitude G and duration δ. With the diffusion time Δ the signal of one component follows the decay $M_{xy}(t) = \frac{1}{2} M_{xy}(0) \times \exp\{-q^2 D\,(\Delta - \delta/3\,)\} \times \exp\{-\Delta\,/T_1\} \times \exp\{-t_E\,/T_2\}$
- Instead of successive Fourier and Laplace transformations a dedicated DOSY transformation provides better inversion stability
- Slices through diffusion peaks of the DOSY map $S(D,\delta)$ parallel to the chemical shift axis δ produce separate spectra for molecules with distinct diffusion coefficients D
- DOSY can be understood as a non-destructive form of *spectral editing* by fractionation through diffusion

Depth Profiling with the NMR-MOUSE

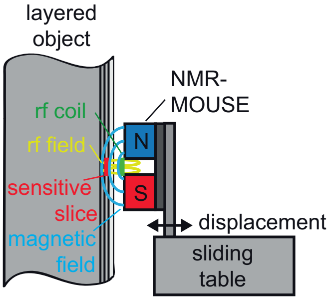

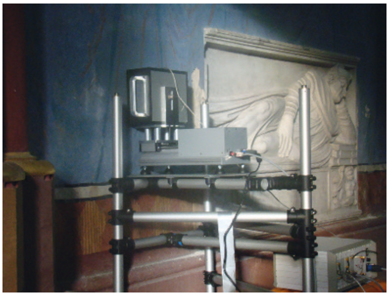

Depth profiles of volumetric moisture content into a wall of the Chapel of St. Mary in Chaalis

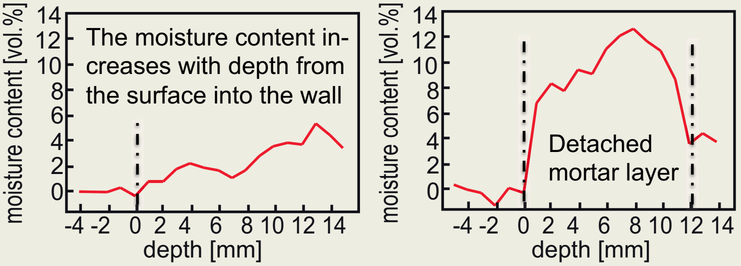

Depth Profiling

- The *NMR-MOUSE* (MObile Universal Surface Explorer) is a *stray-field NMR relaxometer* with a thin, flat slice, which defines the sensitive volume at a fixed distance up to 25 mm away from the surface of the device
- The spins in the sensitive slice produce the NMR signal
- Typically CPMG-type multi-echo trains are measured at different distances of the sensor surface from the object surface
- The NMR signal $M_{xy}(t) = \Sigma_i M_{xy,i}(0) \exp\{-t/T_{2\mathrm{eff},i}\}$ is analyzed for relative component amplitudes $x_i = M_{xy,i}(0)/M_{xy}(0)$ and relaxation times $T_{2\mathrm{eff},i}$ to define amplitudes of profiles as a function of depth into the object (1D images)
- The initial magnetizations $M_{xy,i}(0)$ can be sensitized to diffusion or longitudinal relaxation by means for suitable pulse sequences preceding signal detection
- For fluids in porous media, the initial amplitude of the echo envelope gives *volumetric fluid content* when normalized to the amplitude of the bulk fluid
- The normalized integral of the *CPMG echo envelope* defines a spin-density weighted *average relaxation time*, ${}_0\int^{\infty} M_{xy}(t)\,\mathrm{d}t \,/\, M_{xy}(0) = \Sigma_i\, x_i\, T_{2\mathrm{eff},i} = \langle T_{2\mathrm{eff}} \rangle$
- The empirical *weight function* $w = (t_2-t_1)/t_1 \; {}_0\int^{t_1} M_{xy}(t)\,\mathrm{d}t \,/\, {}_{t_1}\int^{t_2} M_{xy}(t)\,\mathrm{d}t$ provides good contrast as depth-profile amplitude at favorable signal-to-noise ratio

Droplet Size and Solid-Fat Content

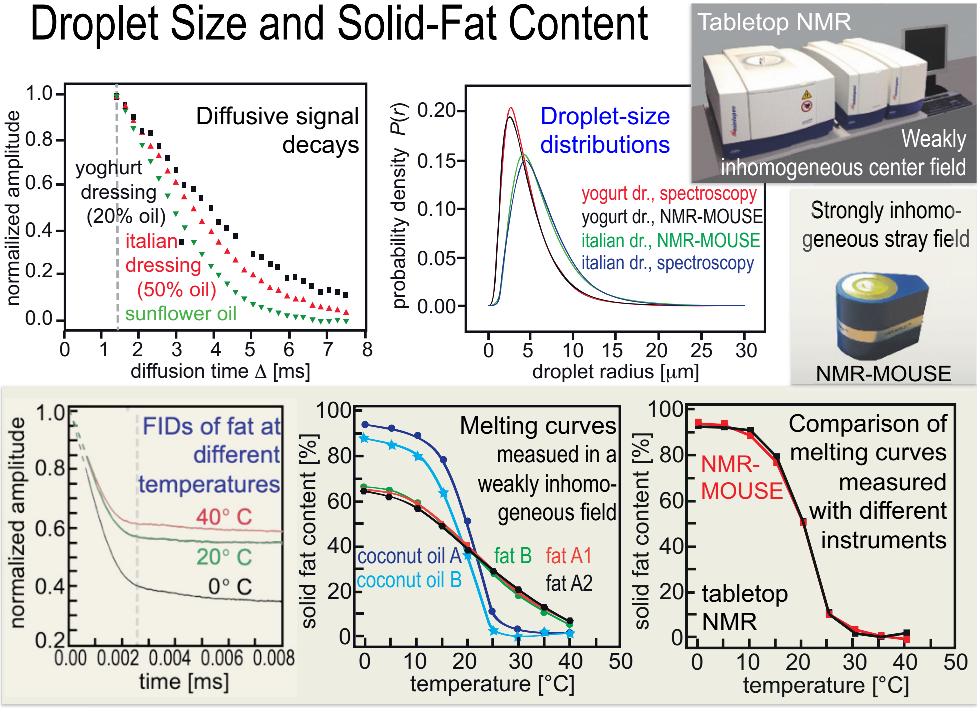

From B. Blümich, S. Haber-Pohlmeier, W. Zia, *Compact NMR*, **de Gruyter**, Berlin, 2014, Fig. 4.3.2 with permission

Emulsions and Suspensions

- *Emulsions* are mixtures of immiscible fluids, where one phase is dispersed as droplets in another continuous phase. Examples are mixtures of oil and water like milk, salad dressing, and skin cream
- In strong field gradients the signal from the freely diffusing molecules decays fast, so that for oil-in-water emulsions, the oil signal survives the water signal
- After 1 to 2 ms diffusion time Δ in a stimulated echo sequence, the water signal in salad dressing has decayed in the stray-field gradient of the order of 20 T/m from the NMR-MOUSE, and the decay of the surviving signal is dominated by the *restricted diffusion* in the more viscous oil droplets
- The decay observed as a function of the diffusion time Δ is typically fitted with a decay modeled for a logarithmic Gaussian *droplet-size distribution*
- *Suspensions* are solid particles suspended in a liquid. They are found in processed food and fat
- The FID from the solid decays fast, that from the liquid much slower
- NMR relaxometry is an official method to determine the *solid fat content*, which specifies the ratio of protons from solid fat to those from total fat
- With the *indirect method*, the amount of liquid fat is given by the room-temperature amplitude of fat at 25 μs deadtime, and the amount of total fat by the signal amplitude at elevated temperature of 60° C where all fat is molten

Skin and Plants

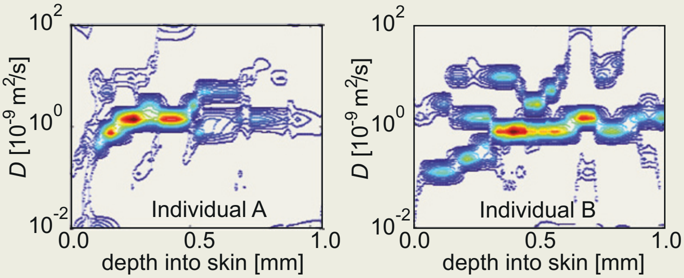

Depth-resolved distributions of diffusion coefficients of the skin from the palm of the hand vary considerably between individuals

From B. Blümich in: G.A. Webb, ed., *Mod. Magn. Reson.*, **Springer**, Cham, DOI 10.1007/978-3-319-28275-6_75-1, Fig. 7 with permission

Cherry tomato plant in a center-field Halbach magnet

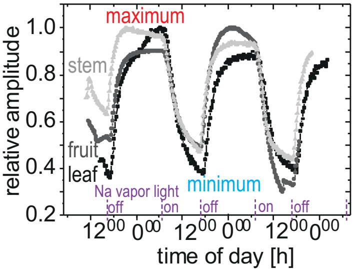

Variation of moisture content in stem, fruit and leaf with artificial illumination

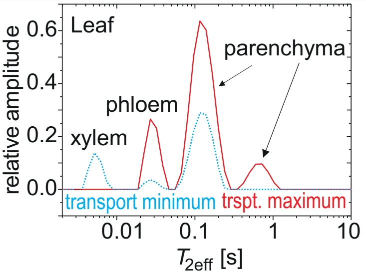

Distributions of relaxation times in the transport maximum and minimum

From D. Oligschläger, C. Rehorn, S. Lehmkuhl, M. Adams, A. Adams, B. Blümich, **J. Magn. Reson. 278** (2017) 80, Figs. 4, 5 with permission

Biological Tissues

- *Biological tissues* are assemblies of cells, which are found in animals and plants
- The most important application of NMR is the study of *human tissue* by *MRI*
- The *contrast* in medical MRI is largely determined by spin density, relaxation times and diffusion coefficients, which are all accessible with Laplace NMR
- The *NMR-MOUSE* has been modified to work with a 2 mm thick sensitive slice with a homogeneous gradient for frequency encoding of depth
- This version has been employed to measure depth-resolved distributions of diffusion coefficients through human *skin*. They bear the characteristic signature of the individual
- With a simple permanent center-field magnet, small *plants* can be studied and the water in the pant tissue be characterized
- The amount of water in different parts of the plant is given by the NMR signal amplitude
- The water transport is high when it is dark and the light stress is off
- *Distributions of relaxation times* measured in the water-concentration extrema during the dark and bright periods identify different locations of the water in the plant tissue

Elastomers are
cross-linked
rubber molecules

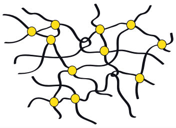

Relaxometry of Cross-Linked Rubber

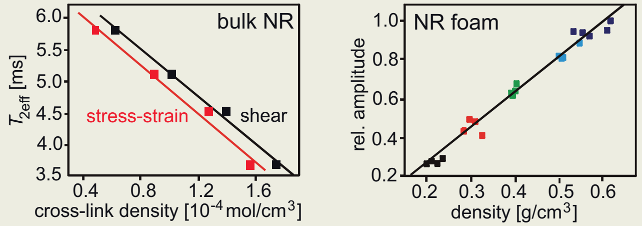

Relaxation maps cross-link density Amplitude maps gravimetric density

From J. Kolz, J. Martins, K. Kremer, T. Mang, B. Blümich, **KGK 60** (2009) 179, Figs. 7, 8 with permission

Transverse magnetization decays map cross-link density via relaxation time and gravimetric density via signal amplitude. For strained elastomers the decays depend on the orientation of the strain direction in the magnetic field

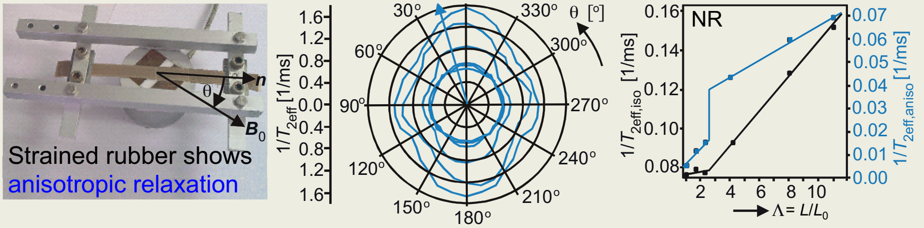

Strained rubber shows anisotropic relaxation

From K. Hailu, R. Fechete, D.E. Demco, B. Blümich, **Solid State Nucl. Magn. Reson. 22** (2002) 327, Fig. 4 with permission

Rubber and Elastomers

- *Rubber* is a melt of entangled macromolecules
- *Elastomers* are chemically crosslinked macromolecules in the molten state
- Sulfur is the most common crosslinking agent
- The chemical crosslinking process is called *vulcanization*
- *Technical elastomers* are statistical products from macromolecules, fillers like carbon black, and processing aids, made by mixing, diffusion, and reaction
- In rubber and elastomers the ^{1}H *relaxation times* are determined by the *chain stiffness* and the *residual dipole-dipole coupling* among ^{1}H nuclei
- A fraction of the dipole-dipole interaction remains unaveraged due to the motional anisotropy of chain segments between entanglements and crosslinks
- At 60 to 80 K above the *glass temperature* T_g the motion is fast, and T_{2eff} is proportional to the *crosslink density* determined by measuring strain and shear
- Closer to T_g the chain stiffness also determines the relaxation times
- The signal amplitude of foamed rubber scales with the *foam density*
- For strained elastomers the relaxation rate depends on the orientation angle
- It is the sum of an isotropic and an anisotropic component. The latter can be approximated by a *Gaussian distribution* of *second Legendre polynomials*
- For NR both relaxation rates change like first-order and second-order phase transitions at the point where *strain-induced crystallization* sets in

Curing, Aging, and Processing

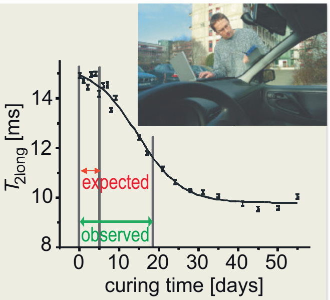

Moisture curing of a windshield adhesive

From K. Kremer, B. Blümich, F.P. Schmitz, J. Seitzer, in: W. Possard, ed., *Adhesion*, **Wiley-VCH**, Weinheim, 2006, p. 435, Figs. 27.5, 27.8 with permission

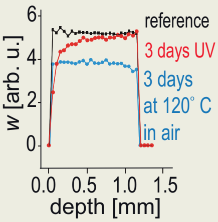

From J. Kolz in: F. Casanova, J. Perlo, B. Blümich, *Single-Sided NMR*, **Springer**, Berlin, 2011, p. 203, Fig. 9.4b with permission

Aging of rubber sheets

Technical elastomers are inhomogeneous materials

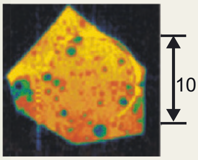

MRI of a technical rubber sample

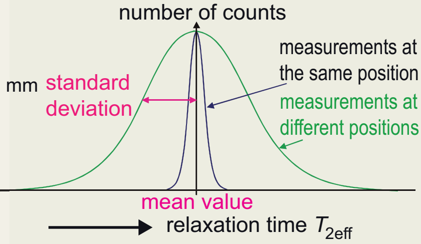

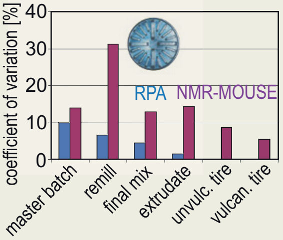

From B. Blümich, A. Buda, K. Kremer, **GAK 6** (2006) 290, Fig. 2 with permission

Properties of Elastomers

- T_{2eff} changes with the *curing time*, e.g. for a moisture-curing poly(urethane) adhesive used for mounting windshields in cars
- Changes in T_{2eff} can be observed well beyond the nominal curing time
- *Aging* of rubber in the presence of oxygen is mostly a combination of chain scission, cross-linking, and oxidation of the polymer
- In many cases the rubber hardens upon *aging*
- *UV aging* affects only the surface of the rubber, while *thermo-oxidative aging* also affects deeper layers
- Technical rubber products are inhomogeneous due to their statistical nature
- Depending on the miscibility of compounds and the processing conditions, some compounds may agglomerate as revealed by *NMR imaging*
- The reproducibility of T_{2eff} in measurements at one point is better than 1 %, but may be worse than 10 % for measurements at different points due to the statistical nature of the material and the small volume of the NMR-MOUSE
- The *NMR-MOUSE* collects signal from a volume element much smaller than the sample size for the rubber process analyzer (RPA), giving rise to a larger coefficient of variation
- For *quality control of rubber products* several measurements need to be conducted at equivalent spots of the product. The mean fit parameters characterize the *average material properties* and the standard deviation the *material heterogeneity*

Non-Destructive Tire Testing

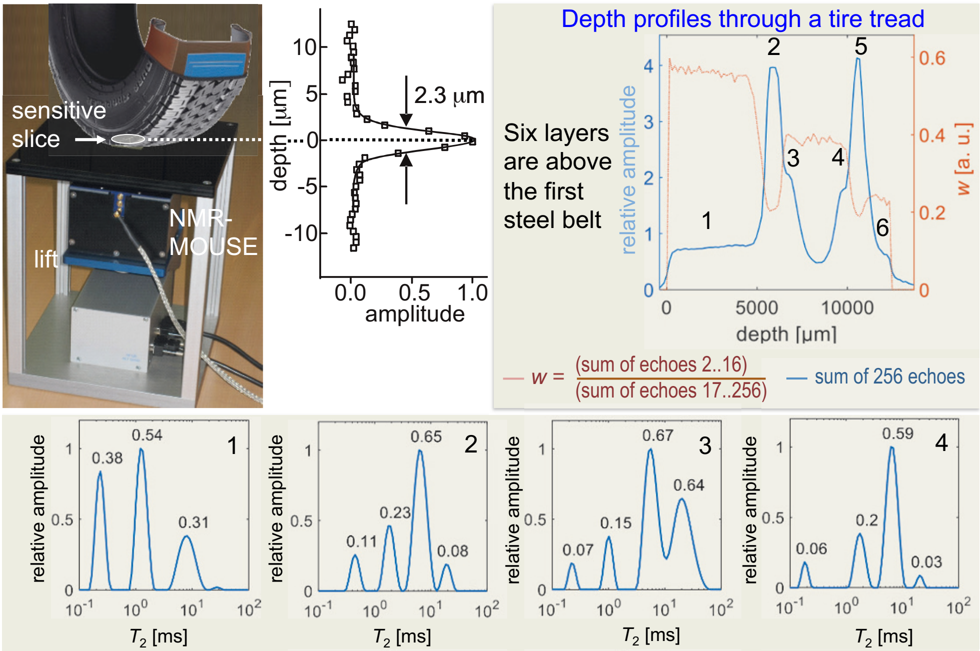

Six layers are above the first steel belt

$w = \frac{\text{(sum of echoes 2..16)}}{\text{(sum of echoes 17..256)}}$

Quality Control of Elastomer Products

- At room temperature, the relaxation times of rubber and elastomers strongly depend on temperature
- For *quality control* of *rubber products*, experimental values of $T_{2\text{eff}}$ need to be extrapolated to a reference temperature and correlated with material properties by means of calibration curves
- *Calibration curves* are determined with small samples in physical testing laboratories by measuring swelling, rheology, and dynamic-mechanical relaxation
- By means of calibration curves NMR relaxation times report parameters like the *glass temperature*, the *elastic modulus*, and the *crosslink density* non-destructively in selected spots from production intermediates and the final product
- A standard application of the NMR-MOUSE is for *tire testing*
- The depth profile of a tire reveals all layers from the tire tread, including the tread base, the steel-belt overlay, and the belt coat up to the first steel belt
- At each depth, the amplitude of the depth profile is calculated in different ways from the *CPMG decay*
- The *distributions of relaxation times* obtained by Laplace transformation of the CPMG decays fingerprint the properties of the material at the given depth

Morphology of Semi-Crystalline Polymers

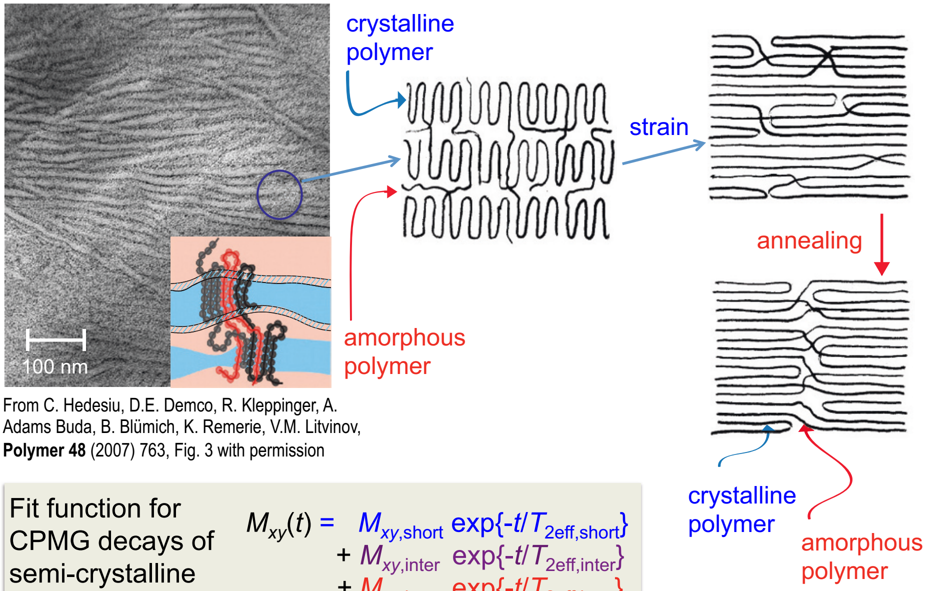

From C. Hedesiu, D.E. Demco, R. Kleppinger, A. Adams Buda, B. Blümich, K. Remerie, V.M. Litvinov, **Polymer 48** (2007) 763, Fig. 3 with permission

Fit function for CPMG decays of semi-crystalline polymers

$$M_{xy}(t) = M_{xy,\mathrm{short}} \exp\{-t/T_{2\mathrm{eff,short}}\} + M_{xy,\mathrm{inter}} \exp\{-t/T_{2\mathrm{eff,inter}}\} + M_{xy,\mathrm{long}} \exp\{-t/T_{2\mathrm{eff,long}}\}$$

Semi-Crystalline Polymers

- *Semi-crystalline polymers* are solids from macromolecules with mobile amorphous and rigid crystalline domains. Sometimes a rigid amorphous interface can be identified by transverse relaxation measurements
- In the *crystalline domains*, the chains are ordered and packed densely, the degrees of freedom for molecular motion are restricted, and T_2 is short
- In the *amorphous domains*, the chains are disordered, the packing density is lower, the motional degrees of freedom are less restricted, and T_2 is longer
- Semi-crystalline polymers like poly(ethylene), poly(propylene), and Nylon, solidify from the melt in lamellar stacks of crystalline and amorphous domains
- Upon drawing, the macromolecular chains realign
- Upon annealing, a fibrillar structure forms with alternating layers of chain-folded lamellae and amorphous domains arranged perpendicular to the drawing direction
- Depending on the temperature history and the shear fields applied during processing, different overall *crystallinity*, different size distribution of the crystallites, and different order in the amorphous domains are generated
- A crude fit to the *transverse relaxation decay* of such polymers is a *tri-exponential function*, where the rapidly, intermediate and slowly relaxing components are assigned to the crystalline, the interfacial and the amorphous domains, respectively

The Impact of Temperature on PE

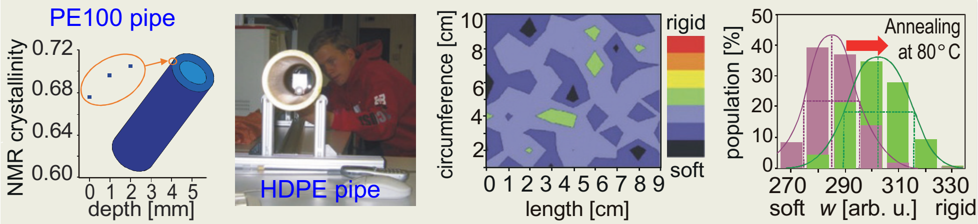

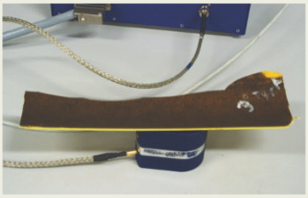

LDPE steel-pipe shell aged 20-30 years in the ground

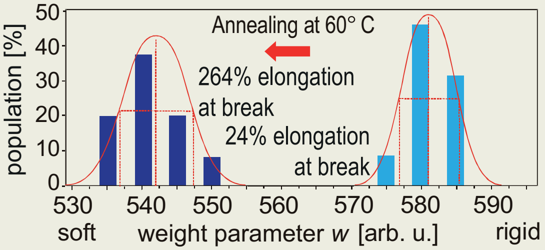

From B. Blümich, A. Adams-Buda, M. Baias, **GWF Gas Erdgas 148** (2007) 95, Figs. 2, 3, 4 with permission

Heterogeneity and Annealing of PE

- *Polymer products* are inhomogeneous for a number of reasons
- They are made from macromolecules with distributions in molecular porperties such as molecular weight, branching, and copolymer statistics
- Polymer processing often involves cooling from the melt. Rapid cooling at the surface leads to lower crystallinity than slow cooling inside the bulk
- In semi-crystalline polymers also the domain sizes are distributed
- The transverse relaxation decays contain signal contributions from crystalline, interfacial and amorphous domains
- The rapidly decaying signal from the crystalline domains is partially lost in the deadtime of the NMR instrument
- A higher value of the *weight parameter w* extracted from the CPMG decay indicates more rigid material or higher crystallinity
- In a melt-extruded HDPE pipe the *crystallinity* increases from the surface to the interior due to the temperature gradient during cooling
- The small sensitive volume of the NMR-MOUSE maps fluctuations in crystallinity. Their distribution shifts to higher crystallinity upon annealing for 24 h at a temperature of 80° C well below the melting temperature of 136° C
- An old LDPE steel-pipe shell has become brittle due to chemical corrosion. The elastic properties could be restored by annealing for 24 h at a temperature of 60° C

Deformation of PE Pipes

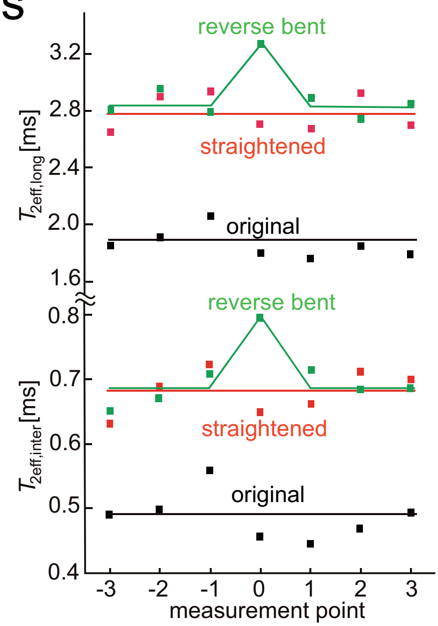

From A. Adams, M. Adams, B. Blümich, J.H. Kocks, O. Hilgert, S. Zimmermann, **3R Int. 49** (2010) 216, Figs. 8, 20 with permission

Mechanical Properties of Semi-Crystalline Polymer Materials

- The *mechanical properties* of semi-crystalline polymer materials are usually explained in terms of the degree of *crystallinity*
- This is so, because crystallinity can easily be determined by *X-ray diffraction* and thermo-analytical methods, whereas NMR is a less common method
- In contrast to X-ray diffraction, NMR relaxation directly measures the signal from the *amorphous domains*
- At small loads in the linear regime of the *stress-strain curve*, deformations are reversible and largely affect only the amorphous but not the crystalline domains
- This is evidenced by the changes in relaxation time $T_{2\text{eff}}$ of a slightly curved, carbon-black filled section of *water pipe* cut from a pipe delivered on a large spool
- Upon bending the section straight, the $T_{2\text{eff}}$ values of the amorphous and interface domains change over the whole length of the pipe section but not those of the crystalline domains
- Upon bending the section in reverse over a pin, the relaxation times of the amorphous and interface domains change only locally at the site of the pin

Physical and Chemical Aging of LDPE

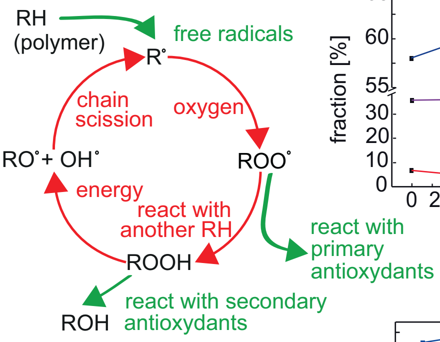
RH (polymer)

free radicals

R°

chain scission

oxygen

RO° + OH°

ROO°

energy

react with another RH

ROOH

react with primary antioxydants

react with secondary antioxydants

ROH

Thermo-oxidative aging at 100° C

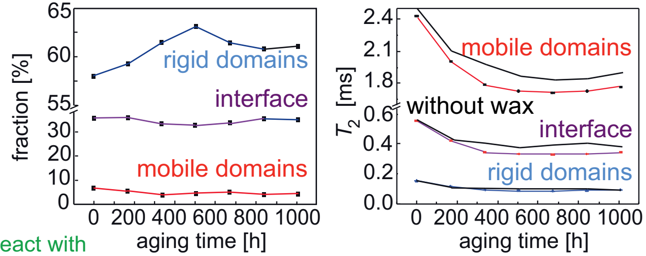

From Y. Teymouri, R. Kwamen, B. Blümich, **Macromol. Mat. Eng. 300** (2015) 1063, Figs. 1, 4 with permission

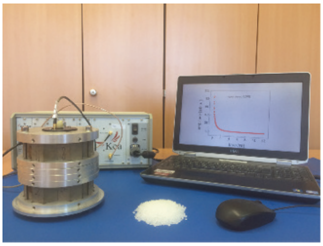

Solvent-induced crystallization (hexane)

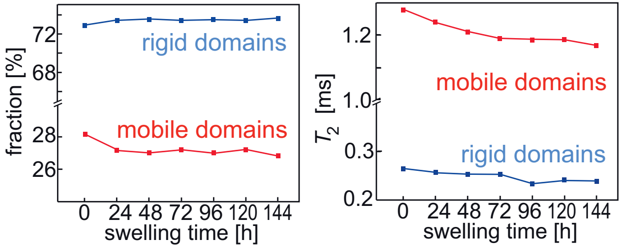

From Y. Teymouri, A. Adams, B. Blümich, **European Polymer J. 80** (2016) 48, Fig. 4 with permission

Aging of Semi-Crystalline Polymers

- *Aging* of *semi-crystalline polymer*s involves at least two competitive processes: *Physical aging* (*crystallization*) and *chemical aging* (*corrosion*)
- A third process can be the loss of low molecular weight compounds by evaporation and leaching through *solvent exposure*
- During *thermo-oxidative aging* the material is exposed to elevated temperature in air
- At short aging times the material predominantly crystallizes so that the fraction of crystalline domains increases, and the mobility, i.e. T_2, of the amorphous domains decreases
- At longer aging times, chemical *degradation* dominates along with chain scission causing the rigid fraction to decrease and the mobility in the amorphous domains to increase
- *Wax* is generated in most polymerization processes as evidenced by the number fraction in the *Schulz-Flory distribution* of molecular weights
- The presence of wax accelerates the physical aging process
- Solvents are taken up essentially only by the amorphous domains in semi-crystalline polymers
- The chain mobility gained by the amorphous chains upon swelling leads to *solvent-induced crystallization* reminiscent of *temperature-induced crystallization*. This process may be impacted by the leaching of wax

Paintings

On wood

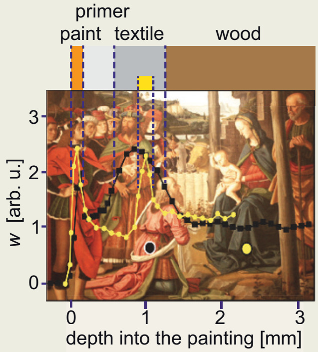

From F. Presciutti J. Perlo, F. Casanova, et al., **Appl. Phys. Lett. 93** (2008) 033505, Fig. 2, doi 10.1063/1.2963026 with permission

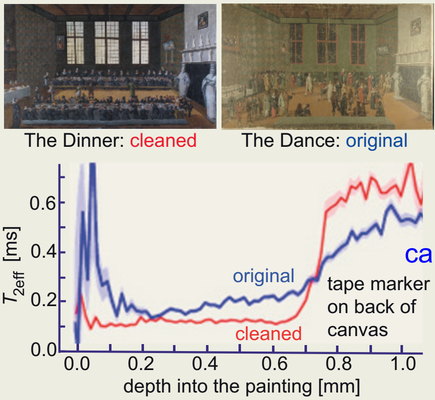

On canvas

From G. Fife, B. Stabik, A.E. Kelley, et al., **Magn. Reson. Chem. 53** (2015) 58, Figs. 1, 3 with permission

On walls

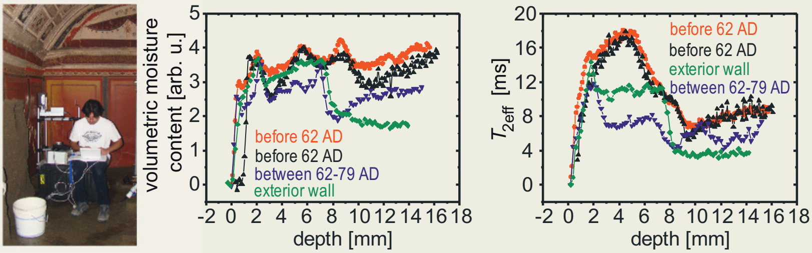

From A. Haber, B. Blümich, D. Souvorova, E. Del Federico, **Anal. Bioanal. Chem. 401** (2011) 1441, Fig. 4 with permission

Cultural Heritage

- Non-destructive testing by stray-field relaxation and diffusion NMR finds more and more applications for studying objects of value to *cultural heritage*
- A proton density higher than expected in depth profiles often indicates the presence of a *conservation agent* like wax in mortar or varnish in bones
- The *stratigraphy of paintings* reveals the thickness of planar layers with an accuracy of 10 μm and material properties from relaxation times and diffusion constants
- For example, in the 1473 AD painting on wood 'Adoration of the Magi' by Perugino, depth profiles at two spots showed a thicker textile layer at the joint between two wooden boards than elsewhere
- The paintings 'The Dinner' and 'The Dance' from the 'Pipenpoyse Wedding' were made in 1616. One was restored and solvent cleaned, the other never restored. $T_{2\text{eff}}$ depth profiles through the paint and canvas regions reveal low $T_{2\text{eff}}$ throughout for the cleaned painting and higher $T_{2\text{eff}}$ for the original painting at deeper depth, suggesting differences in leaching of low molecular weight constituents by *solvent cleaning* and *evaporation*, respectively
- *Frescoes* are painted on wet *mortar* applied in strata of finer and finer grain size towards the surface. The *moisture distribution* across the mortar layers reports the manufacturing technology and skills of the trade from former times such as in the walls of the Villa of the Papyri in Herculaneum